Geochemistry Geophysics Geosystems G3
AN ELECTRONIC JOURNAL OF THE EARTH SCIENCES
Published by AGU and the Geochemical Society

Article
Volume 5, Number 5
21 May 2004
Q05006, doi:10.1029/2003GC000641
ISSN: 1525-2027

Geomagnetic dipole moment and ^{10}Be production rate intercalibration from authigenic ^{10}Be/^{9}Be for the last 1.3 Ma

Julien T. Carcaillet, Didier L. Bourlès, and Nicolas Thouveny

Centre Européen de Recherche et d'Enseignement de Géosciences de l'Environnement, Europôle Méditerranéen de l'Arbois, BP 80, F-13545 Aix en Provence cedex 04, France (carcaillet@cerege.fr; bourles@cerege.fr; thouveny@cerege.fr)

[1] A synthesis of authigenic ^{10}Be/^{9}Be ratio records constructed from sedimentary sequences deposited over the last 300 ka in the North East Atlantic and over the 500–1300 ka BP interval in the West Equatorial Pacific Ocean is compared with proxies of the geomagnetic moment variations over the same time intervals. These proxies consist in (1) relative paleointensity records obtained from the same sediments, (2) a seafloor magnetization record derived from magnetic anomalies, and (3) an absolute Virtual Dipole Moment (VDM) record constructed from an updated database of absolute paleointensities. The authigenic ^{10}Be/^{9}Be ratio records document the occurrence of the paleomagnetic events (excursions and reversals) reported for these time intervals by paleomagnetic studies. Reconstructions of ^{10}Be/^{9}Be derived magnetic moment records based on theoretical and empirical relationships between ^{10}Be/^{9}Be ratio and absolute VDM allow establishing ^{10}Be derived VDM records that exhibit the same overall structures as the geomagnetic proxy records.

Components: 4850 words, 8 figures, 2 tables, 1 dataset.

Keywords: Cosmogenic nuclide production rate; Beryllium; Paleointensity; Geomagnetic moment.

Index Terms: 1040 Geochemistry: Isotopic composition/chemistry; 1521 Geomagnetism and Paleomagnetism: Paleointensity; 1035 Geochemistry: Geochronology.

Received 26 September 2003; **Revised** 28 January 2004; **Accepted** 9 March 2004; **Published** 21 May 2004.

Carcaillet, J. T., D. L. Bourlès, and N. Thouveny (2004), Geomagnetic dipole moment and ^{10}Be production rate intercalibration from authigenic ^{10}Be/^{9}Be for the last 1.3 Ma, *Geochem. Geophys. Geosyst.*, *5*, Q05006, doi:10.1029/2003GC000641.

1. Introduction

[2] Past geomagnetic moment variation are generally evaluated by paleomagnetic methods. However, volcanic materials provide discontinuous records, while sediments, when reliable, yield only relative data. Since cosmogenic nuclide production mainly depends on the geomagnetic moment, high resolution reconstruction of cosmogenic nuclide concentration along sedimentary archives constitute an accurate alternative to document the past magnetic field changes. Indeed, previous studies had shown that major relative paleointensity drops associated with geomagnetic excursions and reversals were accompanied by enhancements of cosmogenic nuclide concentrations [*Raisbeck et al.*, 1985; *Robinson et al.*, 1995; *Wagner et al.*, 2000]. Concentrations of cosmogenic nuclides, and more particularly of ^{10}Be, in marine records being influenced by variations of environmental parameters [*Bourlès et al.*, 1989; *Anderson et al.*, 1990; *Robinson et al.*, 1995], normalisation procedures are required. Therefore a high resolution study of the authigenic ^{10}Be/^{9}Be ratio has been combined

with relative paleointensity determination on sedimentary sequences from Eastern Atlantic and West Equatorial Pacific covering the last 300 ka and the interval 500–1300 ka BP, respectively [*Carcaillet et al.*, 2003, 2004].

[3] Authigenic $^{10}Be/^{9}Be$ variations and absolute VDM must be inter-calibrated in order to reconstruct a cosmogenic nuclide derived VDM record and, reciprocally, to reconstruct atmospheric ^{10}Be production rate variations using an updated database of absolute VDM values.

2. Material and Methods

[4] Clayey-mud and carbonate ooze deposited in the North Eastern Atlantic (MD95-2040, MD95-2042, MD01-2440G) during glacials and interglacials of the last 300 ka, and hemipelagic clayey carbonate ooze deposited in the West Equatorial Pacific (MD97-2140) over the last 1.3 Ma have been sub-sampled for chemical analysis (Table 1). Their chronostratigraphies based on radiocarbon, $\delta^{18}O$ data and reversals magnetostratigraphy extensively presented in [*Carcaillet et al.*, 2003, 2004; *Thouveny et al.*, 2004] yield sedimentation rates of 1.75 cm/ka (MD97-140), 13 cm/ka (MD95-2042) and 7.5 cm/ka (MD95-2040).

2.1. Chemical Procedures

[5] ^{10}Be concentrations measured in marine sediments do not only depend on ^{10}Be production rates but also on environmental conditions affecting the chemical and granulometric composition of the sediments [*Bourlès et al.*, 1989; *Anderson et al.*, 1990; *Robinson et al.*, 1995]. Namely, the absolute ^{10}Be concentration of marine sediments is inversely proportional to their carbonate contents [*Southon et al.*, 1987; *Henken-Mellies et al.*, 1990], and proportional to the specific surface of the settling particles which implies that the total ^{10}Be absolute concentration is meaningless. In order to account for those environmental effects, normalization procedures using either ^{9}Be or $^{230}Th_{xs}$ concentrations are thus required. Since Th is scavenged strongly by carbonate and lithogenic material but weakly by opal, while Be, by contrast, is scavenged strongly by opal and lithogenics but weakly by carbonates, the $^{10}Be/^{230}Th_{xs}$ is composition-dependent [*Chase et al.*, 2002]. Authigenic $^{10}Be/^{9}Be$ ratio thus presently appears to be the appropriate proxy of the ^{10}Be production rate.

[6] We extracted the authigenic (i.e., adsorbed onto particles from the water column) $^{10}Be/^{9}Be$ from the sediments, since only the soluble form of both beryllium isotopes may have been homogenized in the water column before deposition in the sediment [*Bourlès et al.*, 1989; *Robinson et al.*, 1995]. The leaching technique used avoids attacking the lithogenic phase and yields to authigenic $^{10}Be/^{9}Be$ ratios equal to that of the overlying seawater at the time of deposition [*Bourlès et al.*, 1989].

[7] To ensure a representative assay, 2 to 3 grams of oven-dried sediment were crushed. Authigenic ^{10}Be and ^{9}Be were extracted from ~0.5 g subsamples using a 0.04M $NH_2OH.HCl$ in 25% acetic acid leaching solution at 95°C ± 5 during 7 hours [*Bourlès et al.*, 1989]. An aliquot of each sample solution was taken for furnace atomic absorption spectrophotometry determination of ^{9}Be using the method of standard additions and a Zeeman effect background correction (Hitachi Z-8200). Uncertainties in ^{9}Be concentrations are based on the reproducibility of measurements when more than one has been made, or estimated from the best-fit line for reference samples in the case of a single measurement. The remainder of the sample was spiked for isotope dilution with 0.3 g of a 10^{-3} g/g ^{9}Be solution and then purified for ^{10}Be measurements by series of solvent extractions in the presence of EDTA, followed by alkaline (pH ~8) precipitation of $Be(OH)_2$ which is fully converted in BeO by heating at 1000°C.

[8] $^{10}Be/^{9}Be$ ratio measurements performed at the Tandetron AMS facility in Gif-sur-Yvette [*Raisbeck et al.*, 1987, 1994] were calibrated directly against $^{10}Be/^{9}Be$ of the National Institute of Standards and Technology (NIST) standard reference material SRM 4325. The ^{10}Be uncertainties have been estimated using a conservative 5% instrumental uncertainty together with one

Table 1. Geographical Location and Coring Depth of the Studied Cores

Cores	Region	Location	Latitudes	Longitudes	Water Depth	Number of Values
MD0124-40G	Portugese margin, eastern Atlantic	Tagus Continental Rise	37°48N	10°10W	3146	8
MD95-2040	Portugese margin, eastern Atlantic	East Oporto Seamount	40°35N	9°52W	2465	84
MD95-2042	Portugese margin, eastern Atlantic	Tagus Continental Rise	37°48N	10°10W	3146	87
MD97-2140	North New Guinea, western equatorial Pacific	Eauripik Ridge	02°03N	141°46E	2547	81

standard deviation statistics of the number of ^{10}Be events counted (less than ±3%).

3. Authigenic ^{10}Be/^{9}Be Ratios and Relationship With Paleomagnetic Proxies

3.1. Authigenic ^{10}Be/^{9}Be Variability

[9] The results briefly discussed in this section are fully detailed in *Carcaillet et al.* [2003, 2004].

[10] Decay corrected authigenic ^{10}Be concentrations range from 3.46 ± 0.19 10^{-15} to 11.10 ± 0.58 10^{-15}g/g (mean = 7.30 10^{-15}, σ = 1.53 10^{-15}) and authigenic ^{9}Be concentrations from 1.45 ± 0.02 10^{-7} to 1.48 ± 0.06 10^{-6}g/g in the N. E. Atlantic sedimentary sequences. In the West Equatorial Pacific sequence, decay corrected authigenic ^{10}Be concentration range from 7.12 ± 0.49 10^{-15} to 16.78 ± 0.87 10^{-15}g/g (mean = 11.85 10^{-15}, σ = 2.11 10^{-15}) and authigenic ^{9}Be concentrations from 8.16 ± 0.7 10^{-8} to 2.14 ± 0.09 10^{-7}g/g.

[11] Derived authigenic ^{10}Be/^{9}Be ratio thus range from 0.42 ± 0.03 to 5.18 ± 0.31 10^{-8} in the N. E. Atlantic and from 4.94 ± 0.27 to 11.38 ± 0.97 10^{-8} in the West Equatorial Pacific studied sediments. These data show that the difference between the computed authigenic ^{10}Be/^{9}Be values mainly results from the variability of authigenic ^{9}Be concentrations. The significantly higher authigenic ^{10}Be/^{9}Be values observed in the West Equatorial Pacific are in agreement with a weaker continental contribution in that region compared to the N. E. Atlantic, as evidenced by ^{9}Be budgets computed for the respective basins [*Peng et al.*, 1990; *Kusakabe et al.*, 1991] and by a study of the spatial variability of the authigenic ^{10}Be/^{9}Be ratio [*Bourlès et al.*, 1989].

[12] As a consequence of the link between ^{9}Be and detritic inputs, authigenic ^{10}Be/^{9}Be values are inversely related to sedimentation rates. In order to allow comparison between cores from different sites, authigenic ^{10}Be/^{9}Be ratios have thus been multiplied by the respective sedimentation rate values (^{10}Be/^{9}Be$_{cor}$).

[13] Along each studied sedimentary sequence, significant variations of the authigenic ^{10}Be/^{9}Be are observed. Since environmental and spatial variability have been accounted for, they most likely reflect variations of the cosmogenic ^{10}Be production rate mainly controlled by variations of the geomagnetic moment.

3.2. Link to Paleointensity Variations

[14] Different geomagnetic intensity proxy records (Figures 1a, 1b, 1c, 2a, 2b and 2c) are compared with authigenic ^{10}Be/^{9}Be records (Figures 1d and 2d).

[15] 1. Absolute VDM data (VDM$_{abs}$) obtained by application of Thellier and Thellier derived methods were extracted for the two studied time intervals from the Pint$_{2002}$ paleointensity database (ftp://saphir.dstu.univ-montp2.fr/pub/paleointdb/) and updated by other recently published data (see ancillary material). These two sets of 681 and 208 values are not evenly distributed throughout

[1] The ancillary material is available in the HTML version of the article.

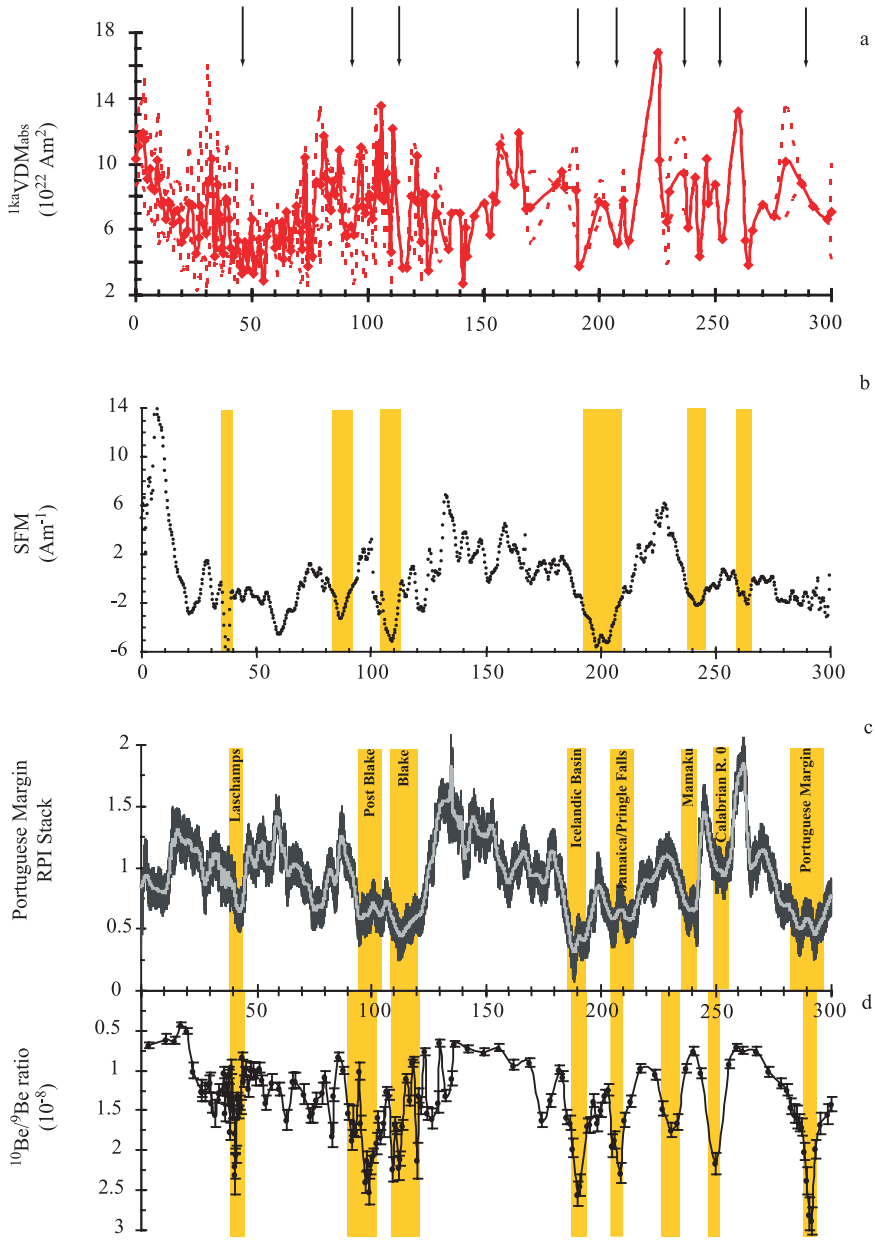

Figure 1. Comparison of paleomagnetic and authigenic ^{10}Be/^{9}Be ratio records between 0 and 300 ka. (a) Absolute VDM (1ka averaged curve, ^{1ka}VDM$_{abs}$) extracted from Pint$_{2002}$ (ftp://saphir.dstu.univ-montp2.fr/pub/paleointdb/) and from other references (see ancillary material)[1]; the dotted curves materialize the 1σ errors when available. (b) Southeast Pacific Sea Floor Magnetization record stacked from eight profiles from the East Pacific Rise 19–20°S [*Gee et al.*, 2000]. (c) Portuguese Margin Relative PaleoIntensity Stack (black curve) and 99% pointwise confidence intervals (gray lines). (d) Composite ^{10}Be/^{9}Be record (reverse axis) along the N. E. Atlantic sequences (Portuguese Margin: MD95-2040, MD95-2042, MD01-2440G) [*Carcaillet et al.*, 2004]. Yellow bars mark the magnetic events.

the time periods of interest: while the last 120 ka interval is well documented (586 data), the 120–300 ka BP interval only contains a hundred of data. In the time interval covering 500–1300 ka, only two periods are intensively documented: the Brunhes/Matuyama transition with ~50 data between 730 and 830 ka, and the time period around 1 Ma with ~40 values presenting large chrono-

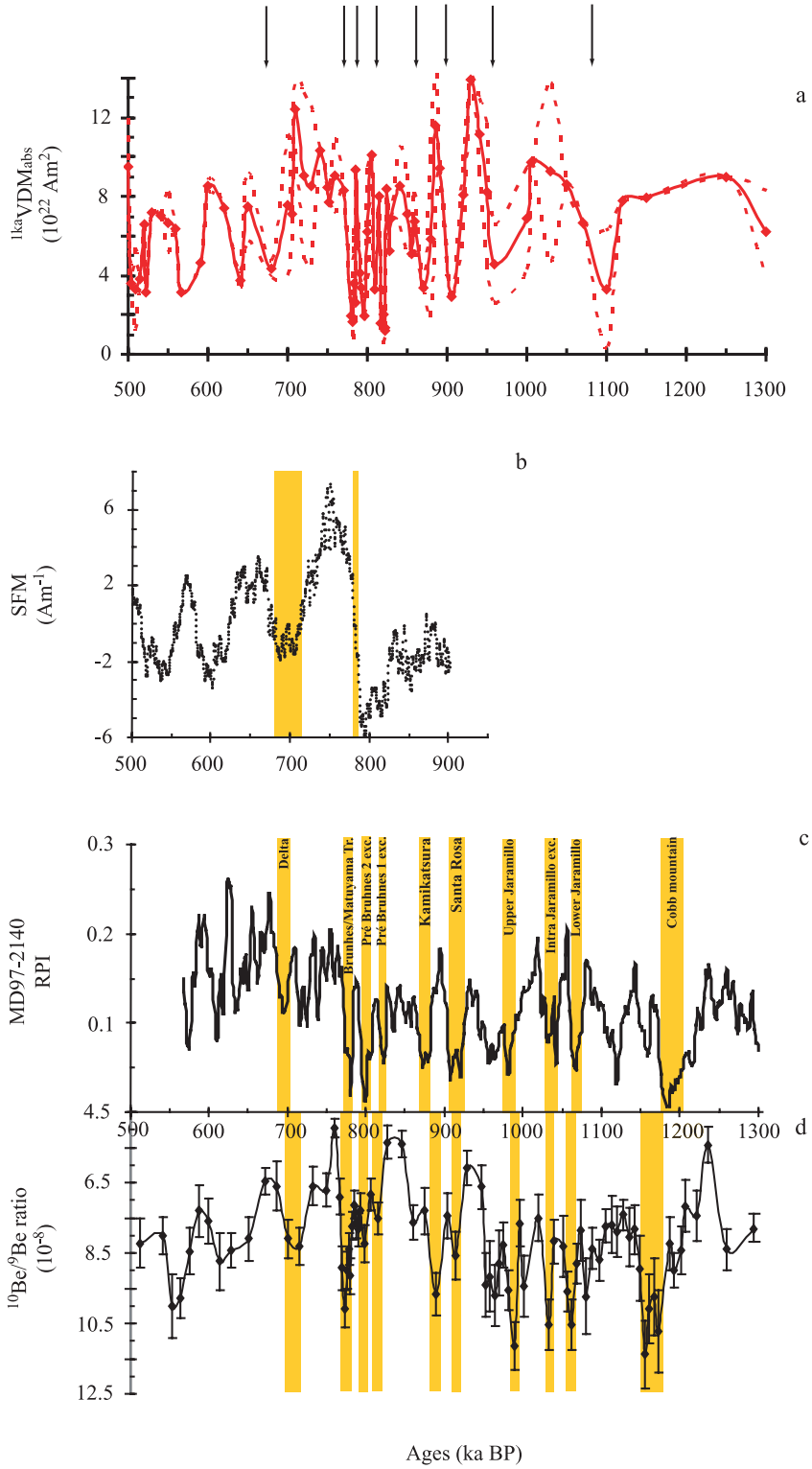

Figure 2. Comparison of paleomagnetic and authigenic ^{10}Be/^{9}Be ratio records between 500 and 1300 ka. (a) Absolute VDM (1 ka averaged curve, ^{1ka}VDM$_{abs}$) extracted from Pint$_{2002}$ (ftp://saphir.dstu.univ-montp2.fr/pub/paleointdb/) and from other references (see ancillary material)[1]; the dotted curves materialize the 1σ errors when available. (b) Southeast Pacific Sea Floor Magnetization record stacked from eight profiles from East Pacific Rise 19–20°S [*Gee et al.*, 2000]. (c) MD97-2140 Relative PaleoIntensity. (d) Authigenic ^{10}Be/^{9}Be record (reverse axis) along MD97-2140 [*Carcaillet et al.*, 2003]. Yellow bars mark the magnetic events.

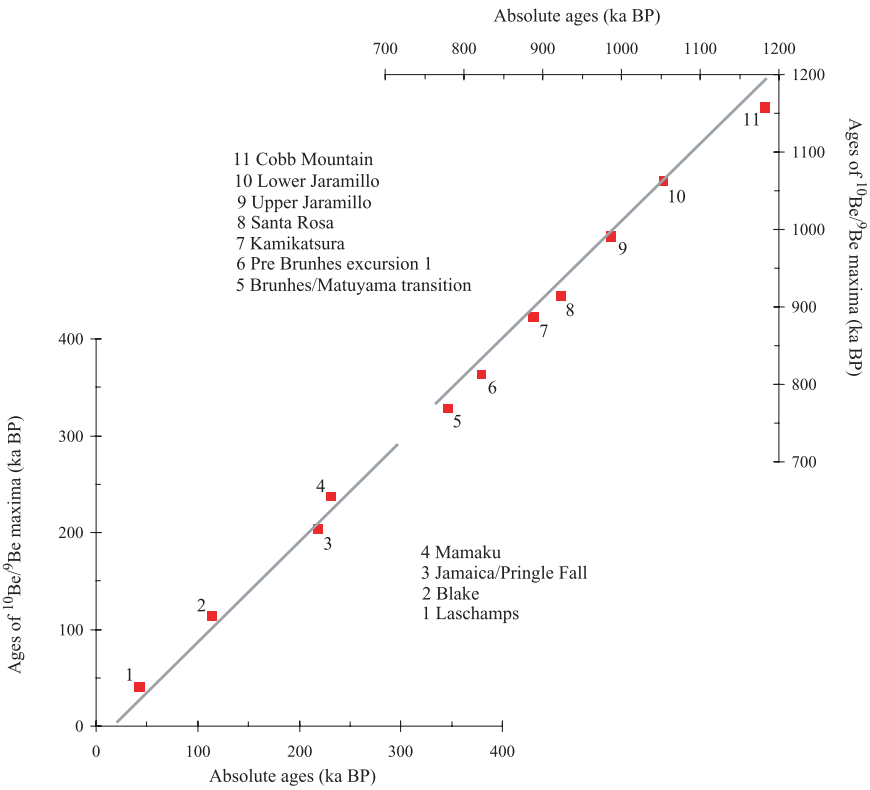

Figure 3. Ages of authigenic $^{10}Be/^{9}Be$ maxima versus absolute ages of magnetic events taken from *Bonhommet and Babkine* [1967] (1), *Fang et al.* [1997] (2), *Herrero-Bervera et al.* [1994] (3), *Shane et al.* [1994] (4), *Singer et al.* [1999] (5, 7, 8, 9, 10, 11), and *Singer et al.* [2002] (6).

logical uncertainties. An average curve was then computed using 1 ka windows in order to reduce the intrinsic variability ($^{1ka}VDM_{abs}$, Figures 1a and 2a).

[16] 2. The South-East Pacific Sea Floor Magnetization record was stacked from eight profiles from the East Pacific Rise 19–20°S [*Gee et al.*, 2000] (SFM, Figures 1b and 2b).

[17] 3. The relative paleointensity records were obtained by normalization of the Natural Remanent Magnetization along the Portuguese Margin sequences (Figure 1c) [*Carcaillet et al.*, 2004; *Thouveny et al.*, 2004] and along the Western Equatorial Pacific core (MD97-2140) [*Carcaillet et al.*, 2003] (Figure 2c).

[18] These paleomagnetic records, issued from diverse paleomagnetic methods, document the occurrence of drastic drops of paleointensities related to geomagnetic excursions or reversals during which authigenic $^{10}Be/^{9}Be$ ratios are systematically enhanced. Along both studied intervals, this direct relationship is supported by an excellent fit between the age of $^{10}Be/^{9}Be$ maxima and absolute ages of magnetic events (Figure 3).

4. Calibrating an Absolute VDM Record

[19] The Elsasser [*Elsasser et al.*, 1956] model linking the ^{14}C production rate (P) to the geomagnetic moment (M), is expressed by the equation, $P(t) = C/(M(t))^{0.52}$, reassessed as $(P/P_0 = M/M_0)^{-1/2}$ by Lal [*Lal*, 1988], $(P/P_0 = M/M_0)^{-1/2}$. Records of relative Virtual Dipole Moment (rVDM) had been derived using the measured $^{10}Be/^{9}Be$ ratios [*Carcaillet et al.*, 2003, 2004]. Comparison of these rVDM records with the VDM_{abs} revealed common features [*Carcaillet et al.*, 2003, 2004]. Since the accuracy of the Elsasser based reconstruction

Table 2. Average Values of Clusters Computed From $^{10}Be/^{9}Be_{cor}$ and $^{1ka}VDM_{abs}$ Data Sets[a]

	VDM	σ		$^{10}Be/^{9}Becor$	σ
MD01-2440G and 952042					
average +1σ	10.33	1.04	average −1σ	9.84	2.55
average ±1σ	6.94	1.14	average ±1σ	17.59	3.12
average −1σ	4.20	0.46	average −1σ	28.02	1.57
MD95-2040					
average +1σ	11.65	1.74	average −1σ	10.32	1.18
average ±1σ	7.55	1.13	average ±1σ	19.91	4.12
average −1σ	4.28	0.69	average −1σ	32.37	3.13
MD97-2140					
average +1σ	10.61	1.51	average −1σ	11.15	1.21
average ±1σ	6.68	1.69	average ±1σ	14.29	1.07
average −1σ	2.55	0.81	average −1σ	17.76	1.01

[a] See ancillary material.

leading to extremely low VDM values is questionable [*Bard*, 1998, Figure 9] and, since our data set contains a great number of high $^{10}Be/^{9}Be$ ratios linked to low VDM values during excursions, we will attempt to construct an empirical relationship between the geomagnetic dipole moment and the cosmogenic nuclide production rate. This relationship will be used to construct (1) an absolute ^{10}Be derived VDM record and (2) a time dependent cosmogenic nuclide production rate record for the 0–300 ka BP and the 500–1300 ka BP intervals.

4.1. Methods

[20] Since cosmogenic nuclide ratios and RPI data sets were obtained from the same sedimentary sequences, they are not independent data sets. Cosmogenic nuclide data were thus calibrated using absolute VDM data obtained and dated by different methodologies.

[21] For each time interval corresponding to the studied cores (MD95-2042/MD01-2440G: 0–140 ka BP; MD95-2040: 65–300 ka BP and MD97-2140: 500–1300 ka), $^{1ka}VDM_{abs}$ data and $^{10}Be/^{9}Be_{cor}$ data were sorted in three clusters defined as (1) the data comprised between +1σ and −1σ around the mean value of all the data; (2) the data higher than the mean +1σ; and (3) the data lower than the mean values −1σ. Mean values and their standard deviations were then computed for each cluster (Table 2).

[22] The physical link between magnetic moment (M) and cosmogenic nuclide production rate (P) being expressed by a power law such as: $P_{(t)} = C/M^{n}_{(t)}$ [*Elsasser et al.*, 1956], the proposed calibration associates mean values of minimum authigenic $^{10}Be/^{9}Be_{cor}$ (Be_{min}) with maximum $^{1ka}VDM_{abs}$ (VDM_{max}); (Be_{max}) with (VDM_{min}); and mid-values (Be_{mid} with VDM_{mid}) (Figure 4).

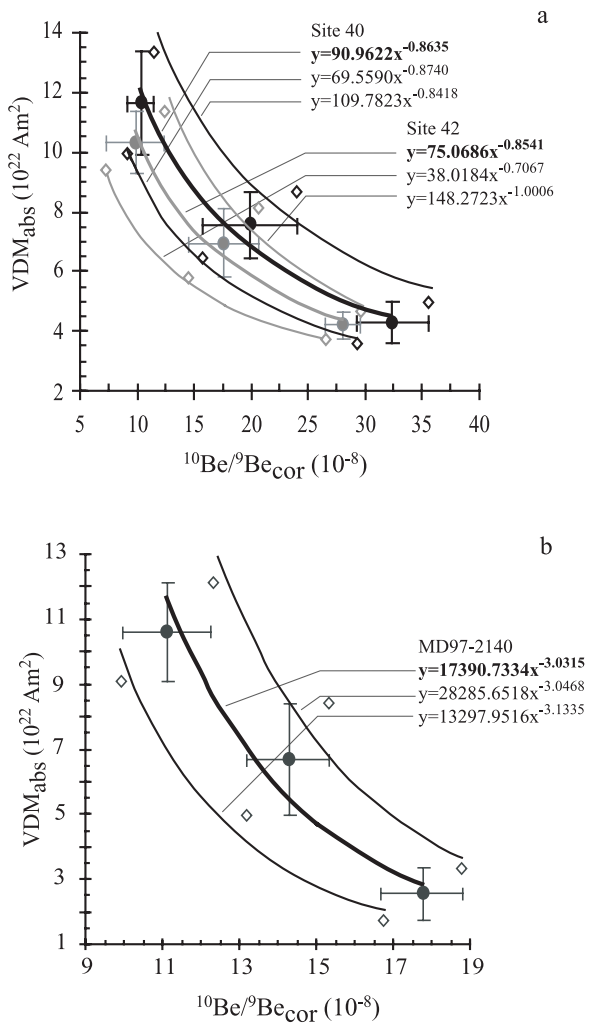

Figure 4. $^{1ka}VDM_{abs}$ as a function of $^{10}Be/^{9}Be_{cor}$ provide best fits through the clusters (see text). (a) Gray circles correspond to MD95-2042/MD01-2440 data set; black circles correspond to MD95-2040 data set. Gray and black diamonds correspond to the best fits computed through the uppermost and lowermost uncertainties, respectively. (b) Black circles correspond to MD97-2140 data set. Black diamonds correspond to the best fits computed through the uppermost and lowermost uncertainties.

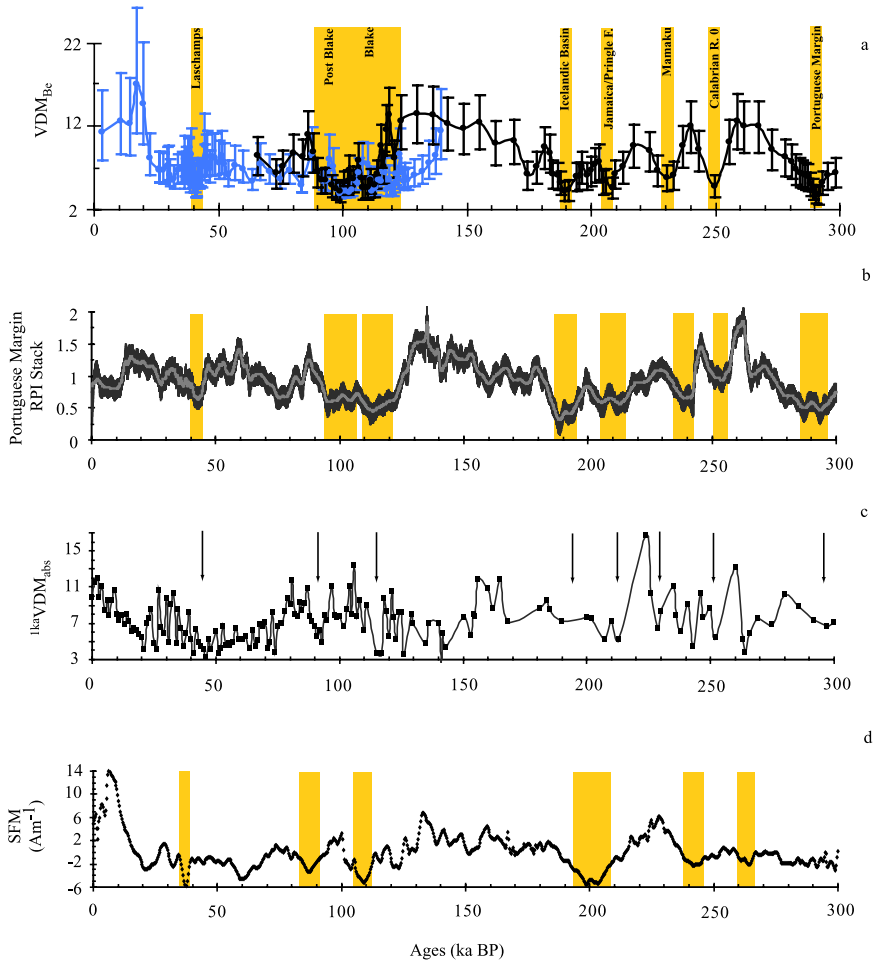

Figure 5. Comparison of proxies of the geomagnetic moment between 0 and 300 ka. (a) VDM_{Be} derived from the model presented (see text), the blue curve and its associated uncertainties are computed using the equations associated to MD95-2042/MD01-2440G, the black curve and its associated uncertainties are computed using the equations associated to MD95-2040 (Figure 4a). (b) Portuguese Margin Relative PaleoIntensity Stack (black curve) and 99% pointwise confidence interval (gray lines). (c) $^{1ka}VDM_{abs}$. (d) Southeast Pacific Sea Floor Magnetization record [*Gee et al.*, 2000]. Names of the excursions have been indicated and emphasized by gray area; arrows on Figure 5c indicate the time of their occurrence and refer to the associated low VDM.

[23] For each sedimentary sequence, the best fit through the relevant series is computed as: $^{1ka}VDM_{abs} = (A*^{10}Be/^{9}Be_{cor})^{-B}$. Linked uncertainties have been computed by fitting: (1) the values corresponding to mean values $+1\sigma$ and (2) the values corresponding to mean values -1σ.

[24] Despite the correction of environmental effects (normalization of authigenic ^{10}Be by authigenic ^{9}Be and multiplication by sedimentation rate), the amplitude of the $^{10}Be/^{9}Be$ response to the VDM forcing appears to be significantly stronger in the N. E. Atlantic sequences than in the West Equatorial Pacific (Figure 4).

4.2. Reconstruction of a VDM Record From Authigenic $^{10}Be/^{9}Be$ Ratios

[25] The equations formerly obtained allow reconstructing from the high resolution authigenic $^{10}Be/^{9}Be_{cor}$ records VDM derived records (VDM_{Be}) (Figures 5a and 6a) that can be compared with paleomagnetic intensity proxy records (Figures 5b, 5c, 5d, 6b, 6c, and 6d). In agreement with these proxy records, the VDM_{Be} records exhibit long

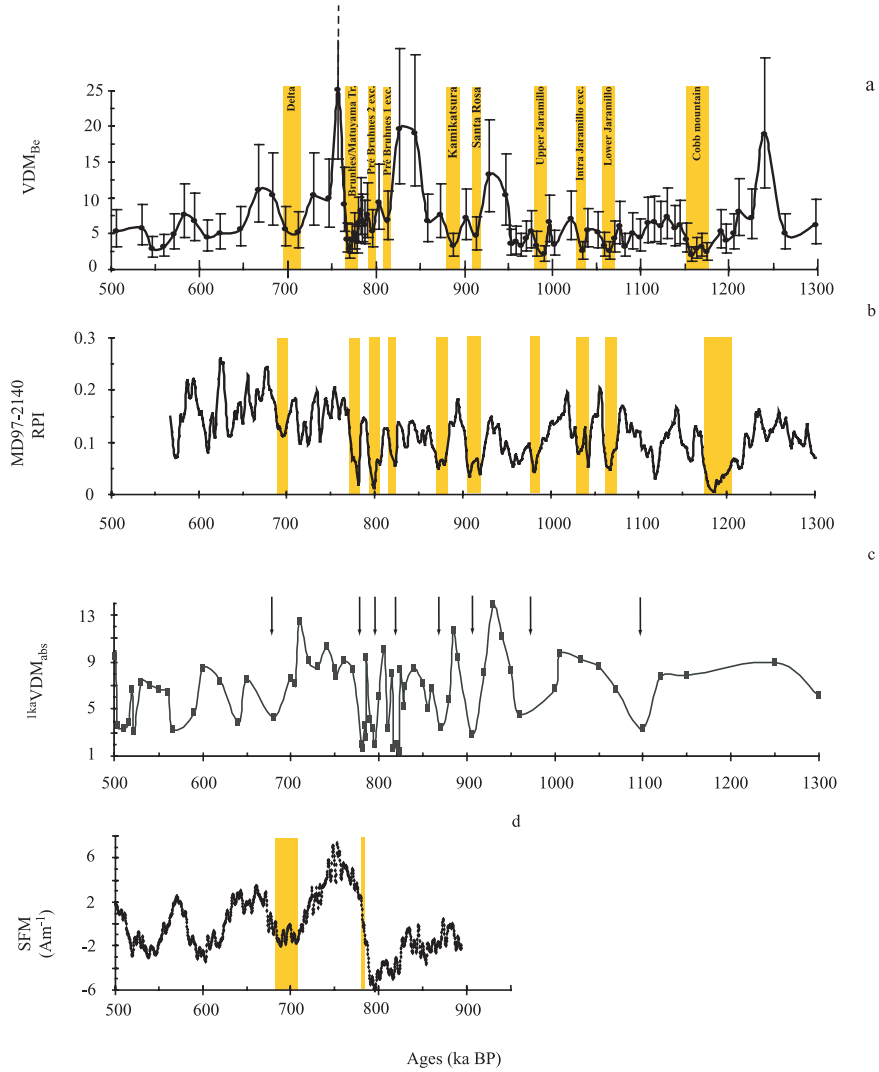

Figure 6. Comparison of proxies of the geomagnetic moment between 500 and 1300 ka. (a) VDM$_{Be}$ and its associated uncertainties are computed from the model presented using the equations associated to MD97-2140 (Figure 4b). (b) MD97-2140 Relative PaleoIntensity record. (c) ^{1ka}VDM$_{abs}$. (d) Southeast Pacific Sea Floor Magnetization record [*Gee et al.*, 2000]. Names of the excursions have been indicated and emphasized by gray area; arrows on Figure 6c indicate the time of their occurrence and refer to the associated low VDM.

lasting low VDM phases corresponding to geomagnetic excursions or reversals.

[26] During the last 300 ka (Figure 5), drops of the VDM$_{Be}$ are assignable to the Laschamps excursion (39–42 ka BP), the Blake event and the post-Blake excursion (both included in the same low VDM interval (89–123 ka BP), the Icelandic Basin (~190 ka BP), the Jamaica/Pringle Falls (205–210 ka BP), the Mamaku excursion (~230 ka BP) and the Calabrian Ridge (~250 ka BP). The occurrence of the new Portuguese Margin excursion [*Thouveny et al.*, 2004] is marked by a drop of the VDM$_{Be}$ and of the RPI at ~290 ka BP, that appears attenuated in the ^{1ka}VDM$_{abs}$ and absent in the SFM record. Within this time interval, the most prominent and long lasting feature of the VDM$_{Be}$ is associated with the Blake event and the post-Blake excursion. With a rapid loss of ~70% of the value prevailing during the preceding time period (125–150 ka BP) and a duration of more than 25 ka, it is the most significant registered drop compared to the other excursions that do not exceed ~60% of loss and do not last more than 10 ka. However,

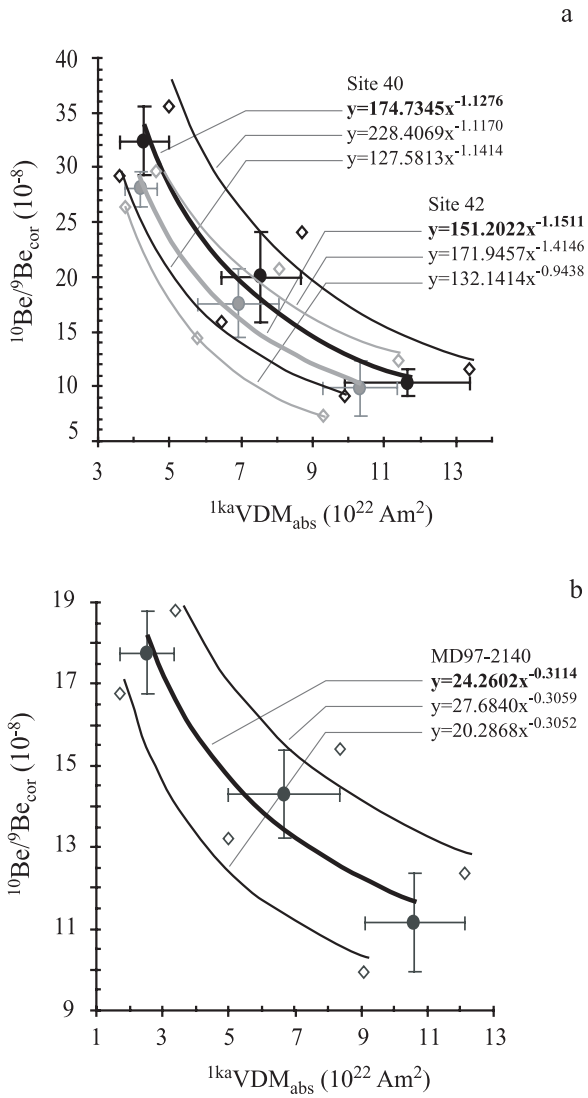

Figure 7. $^{10}Be/^{9}Be_{cor}$ as a function of $^{1ka}VDM_{abs}$ provide best fits through the clusters (see text). (a) Gray circles correspond to MD95-2042/MD01-2440 data set; black circles correspond to MD95-2040 data set. Gray and black diamonds correspond to the best fits computed through the uppermost and lowermost uncertainties, respectively. (b) Black circles correspond to MD97-2140 data set. Black diamonds correspond to the best fits computed through the uppermost and lowermost uncertainties.

while this observation is also valid for the RPI and SFM records, a major discrepancy has to be noted for the interval 90–150 ka BP of the $^{1ka}VDM_{abs}$ that presents dominantly weak values from 150 to 125 ka BP and high values at ~105 ka BP. This emphasizes the necessity for an improvement of both the chronology and the resolution of the absolute VDM record.

[27] Interval 500–1300 ka BP (Figure 6) is dominated by phases of low VDM_{Be}, the minima of which correspond to the lowest RPI values at the time of reversals and excursions. In all presented records, the interval 500–750 ka BP is characterized by the occurrence of three low VDM phases, the oldest (~700 ka BP) being identified as the Delta excursion, and the interval 750–850 ka BP by the occurrence of the Brunhes/Matuyama transition and its two pre-transitional excursions. This last interval yields to the largest amplitude variation (~85%) in the VDM_{Be} [*Carcaillet et al.*, 2003]. The significant drop between 920 and 850 ka BP is assignable to the Kamikatsura and Santa Rosa excursions. Finally, the long phase of low VDM_{Be} (1230–950 ka BP) contains the Upper Jaramillo transition (~990 ka BP), an intra-Jaramillo excursion (~1040 ka BP), the Lower Jaramillo transition (~1070 ka BP) and the Cobb Mountain event (~1200 ka BP). Despite its weak resolution and chronological uncertainties the $^{1ka}VDM_{abs}$ documents most of these important features.

4.3. Reconstruction of the Temporal Variation of Atmospheric ^{10}Be Production Rate

[28] The aim of this section is to use the relationship between authigenic $^{10}Be/^{9}Be$ ratio and VDM_{abs} demonstrated in the previous sections, in order to, by an inverse approach, reconstruct the temporal variations of the atmospheric ^{10}Be production rate from the temporal variations of the geomagnetic dipole moment expressed by the $^{1ka}VDM_{abs}$ record. The statistical approach developed in section 4.1 has been applied to model the inverse relationships $^{10}Be/^{9}Be = (A^* VDM)^{-B}$ (Figure 7). Considering the complexity and poor knowledge of the mechanisms involved in atmospheric and oceanic transfers from the stratosphere to the deep ocean, we performed a calibration of the modeled ^{10}Be production rates setting the present atmospheric ^{10}Be production rate ($^{abs}P_0$) to a global average production rate of 1.

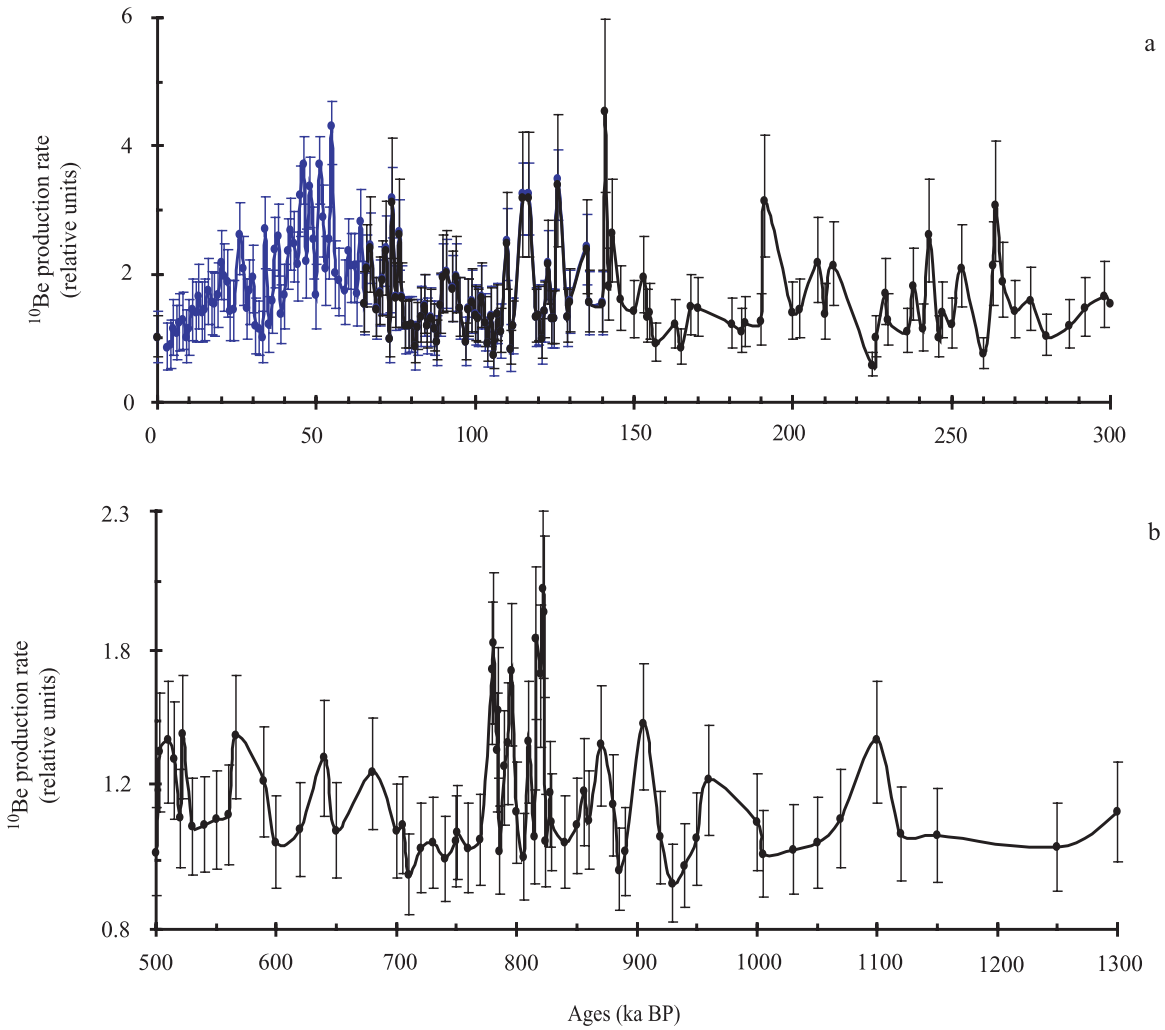

Figure 8. Reconstruction of the temporal variations of the atmospheric ^{10}Be production rate relative to a present global average production rate set to 1. (a) Portuguese margin area. The blue curve and its associated uncertainties are computed using the equations associated to MD95-2042/MD01-2440G. The black curve and its associated uncertainties are computed using the equations associated to MD95-2040 (Figure 7a). (b) West Equatorial Pacific area. The curve and its associated uncertainties are computed using the equations associated to MD97-2140 (Figure 7b).

[29] The reconstructed temporal evolution of the atmospheric ^{10}Be production rate (P) (Figure 8) documents short and long-term variations with P generally higher than the present value. Particularly, for the time period 0–300 ka BP recorded in the N. E. Atlantic area, a long lasting period of significantly enhanced P occurred between ~40 and ~60 ka BP, while shorter episodes of enhancement occurred at ~115, ~125, ~140, ~265 ka BP. For the other time period (500–1300 ka BP) recorded in the equatorial area, significant increases of P are observed between 780 and 830 ka BP, i.e., for the absolute VDM values documenting the low geomagnetic moment linked to the Brunhes/Matuyama transition and its associated excursions.

5. Conclusions

[30] Along Quaternary sedimentary sequences deposited in the context of an excursional and reversing geomagnetic field, authigenic ^{10}Be/^{9}Be

ratios present a temporal variability linked, at the first order, to the strength of the geomagnetic dipole, as evidenced by drastic enhancements of the $^{10}Be/^{9}Be$ ratio during low dipole moment phases. An empirical relationship established between the $^{10}Be/^{9}Be$ ratios and absolute VDM values allowed to construct a ^{10}Be derived VDM record. This new geomagnetic moment proxy record, independent from paleomagnetic methods, confirms the major patterns documented in the other geomagnetic moment proxy records (e.g., relative paleointensity stacks and South East Pacific Sea Floor Magnetization record). Namely, it evidences every major low dipole moment phases associated with excursions or reversals documented by paleomagnetic directions in these or in other studied sequences. It furthermore suggests the predominance of a low geomagnetic dipole regime over the studied time intervals.

[31] The inverse empirical relationship was used to construct a VDM derived atmospheric ^{10}Be production rate record relative to a present global average atmospheric production rate set to 1. Providing a better understanding between the mean global atmospheric production rate of ^{10}Be and in situ production rates, this opens perspectives for the calibration of the temporal evolution of the in situ produced ^{10}Be production rate, and thus for a better accuracy of the deduced cosmic ray exposure ages.

Acknowledgments

[32] We are grateful to D. Lal and an anonymous reviewer for their critics and suggestions which helped to greatly improve the manuscript. We thank M. Arnold for his precious assistance on the Accelerator Mass Spectrometer (Tandétron - Gif/Yvette). This study was funded by the Programme "Intérieur de la Terre" (CNRS-INSU) through the "ISOMAG" Project (N.T. and D.B.).

References

Anderson, R. F., Y. Lao, W. S. Broecker, S. E. Trumbore, H. J. Hofmann, and W. Wolfli (1990), Boundary scavenging in the Pacific Ocean: A comparison of ^{10}Be and ^{231}Pa, *Earth Planet. Sci. Lett.*, *96*, 287–304.

Bard, E. (1998), Geochemical and geophysical implications of the radiocarbon calibration, *Geochim. Cosmochim. Acta*, *62*, 2025–2038.

Bonhommet, N., and J. Babkine (1967), Sur la présence d'aimantations inversées dans la Chaîne des Puys, *C. R. Acad. Sci. Paris*, *264*, 92–94.

Bourlès, D. L., G. M. Raisbeck, and F. Yiou (1989), ^{10}Be and ^{9}Be in marine sediments and their potential for dating, *Geochim. Cosmochim. Acta*, *53*, 443–452.

Carcaillet, J. T., N. Thouveny, and D. L. Bourlès (2003), Geomagnetic moment instability between 0.6 and 1.3 Ma from cosmonuclide evidence, *Geophys. Res. Lett.*, *30*(15), 1792, doi:10.1029/2003GL017550.

Carcaillet, J., D. L. Bourlès, N. Thouveny, and M. Arnold (2004), A high resolution authigenic $^{10}Be/^{9}Be$ record of geomagnetic moment variations over the last 300 ka from sedimentary cores of the Portuguese margin, *Earth Planet. Sci. Lett.*, *219*, 397–412.

Chase, Z., R. F. Anderson, M. Q. Fleisher, and P. W. Kubik (2002), The influence of particle composition and particle flux on scavenging of Th, Pa and Be in the ocean, *Earth Planet. Sci. Lett.*, *204*, 215–229.

Elsasser, W., E. P. Ney, and J. R. Winckler (1956), Cosmic-ray intensity and geomagnetism, *Nature*, *178*, 1226–1227.

Fang, X. M., J. J. Li, R. Van der Voo, C. Mac Niocaill, X. R. Dai, R. A. Kemp, E. Derbyshire, J. X. Cao, J. M. Cao, and G. Wang (1997), A record of the Blake event during the last interglacial paleosol in the western loess plateau of China, *Earth Planet. Sci. Lett.*, *146*, 73–82.

Gee, J. S., S. C. Cande, J. A. Hildebrand, K. Donnelly, and R. L. Parker (2000), Geomagnetic intensity variations over the past 780 kyr obtained from near-seafloor magnetic anomalies, *Nature*, *408*, 827–832.

Henken-Mellies, W. U., J. Beer, F. Heller, K. J. Hsü, C. Shen, G. Bonani, H. J. Hoffmann, M. Suter, and W. Wölfli (1990), ^{10}Be and ^{9}Be in South Atlantic DSDP Site 519: Relation to geomagnetic reversals and to sediment composition, *Earth Planet. Sci. Lett.*, *98*, 267–276.

Herrero-Bervera, E., et al. (1994), Age and correlation of a paleomagnetic episode in the western united states by Ar-40/Ar-39 dating and tephrochronology: The Jamaica, Blake or a new polarity episode?, *J. Geophys. Res.*, *99*, 24,091–24,103.

Kusakabe, M., T. L. Ku, J. R. Southon, S. Liu, J. S. Vogel, D. E. Nelson, S. Nakaya, and G. L. Cusimano (1991), Be isotope in rivers/estuaries and their oceanic budgets, *Earth Planet. Sci. Lett.*, *102*, 265–276.

Lal, D. (1988), Theoretically expected variations in the terrestrial cosmic-ray production rates of isotopes, in *Solar-Terrestrial Relationships*, edited by G. C. Castagnoli and D. Lal, pp. 216–233, Soc. Italiana di Fisica-Bologna-Italy, Bologna.

Peng, T. H., T. L. Ku, J. Southon, C. Measures, and W. S. Broecker (1990), Factors controlling the distribution of ^{10}Be and the ^{9}Be in the ocean, in *Mantle to Meteorites*, edited by K. Gopalan, pp. 201–204, Indian Acad. of Sci., Bangalore.

Raisbeck, G. M., F. Yiou, D. Bourlès, and D. V. Kent (1985), Evidence for an increase in cosmogenic ^{10}Be during a geomagnetic reversal, *Nature*, *315*, 315–317.

Raisbeck, G. M., F. Yiou, D. L. Bourlès, J. Lestringuez, and D. Deboffle (1987), Measurements of ^{10}Be and ^{26}Al with a

Tandetron AMS facility, *Nucl. Instrum. Methods*, *B29*, 22–26.

Raisbeck, G. M., F. Yiou, D. Bourlès, E. Brown, D. Deboffle, P. Jouhanneau, J. Lestringuez, and Z. Q. Zhou (1994), The AMS facility at Gif-sur-Yvette: Progress, perturbations and projects, *Nucl. Instrum. Methods*, *B92*, 43–46.

Robinson, C., G. M. Raisbeck, F. Yiou, B. Lehman, and C. Laj (1995), The relationship between ^{10}Be and geomagnetic field strength records in central North Atlantic sediments during the last 80 ka, *Earth Planet. Sci. Lett.*, *136*, 551–557.

Shane, P., T. Black, and J. Westgate (1994), Isothermal plateau fission-track age for a paleomagnetic excursion in the Mamaku ignimbrite, New Zealand and implication for late Quaternary stratigraphy, *Geophys. Res. Lett.*, *21*(16), 1695–1698.

Singer, B. S., K. A. Hoffman, A. Chauvin, R. S. Coe, and M. S. Pringle (1999), Dating transitionally magnetized lavas of the late Matuyama Chron: Toward a new ^{40}Ar/^{39}Ar timescale of reversal and events, *J. Geophys. Res.*, *104*(B1), 679–693.

Singer, B. S., M. K. Relle, K. A. Hoffman, A. Battle, C. Laj, H. Guillou, and J. C. Carracedo (2002), Ar/Ar ages from transitionally magnetized lavas on La Palma, Canary Island, and the geomagnetic instability timescale, *J. Geophys. Res.*, *107*(B11), 2307, doi:10.1029/2001JB001613.

Southon, J. R., T. L. Ku, D. E. Nelson, J. L. Reyss, J. C. Duplessy, and J. S. Vogel (1987), ^{10}Be in a Deep-sea core: Implications regarding ^{10}Be production changes over the past 420 ka, *Earth Planet. Sci. Lett.*, *85*, 356–364.

Thouveny, N., J. Carcaillet, E. Moreno, G. Leduc, and D. Nérini (2004), Geomagnetic moment variation and paleomagnetic excursions since 400 ka BP: A stacked record of sedimentary sequences of the Portuguese Margin, *Earth Planet. Sci. Lett.*, *219*, 377–396.

Wagner, G., J. Masarik, J. Beer, S. Baumgartner, D. Imboden, P. W. Kubik, H. A. Synal, and M. Suter (2000), Reconstruction of the geomagnetic field between 20 and 60 kyr BP from cosmogenic radionuclides in the GRIP ice core, *Nucl. Instrum. Methods*, *B172*, 597–604.